Proc. of SPIE Vol. 0181, Contemporary Optical Systems & Components Specifications, ed. Robert E. Fischer (Apr 1979) Copyright SPIE

Specifications for diamond-turned surfaces

E. R. Freniere and J. Zimmerman
Honeywell Electro-Optics Center
Lexington, Massachusetts 02173

Abstract

The surfaces of diamond machined optics are described in terms of the spatial frequency of the errors. Certain of these errors which are unique to diamond machined optics, such as, the highly correlated errors due to tool advance and the error due to machine centering uncertainty, are discussed in detail.

The imaging effects of the errors are derived. A framework for specifying diamond machined optics, based on the imaging effects is presented.

Introduction

Diamond turning or single point diamond machining has become an attractive method for producing optical surfaces in production quantities.[1,2] Developments in machine tool design, control systems and measurement techniques have made possible the routine use of diamond machined surfaces in infrared systems. The continuing advance in these technologies gives rise to the expectation of using diamond machined optics in the visible wavelength region. A photograph of a state-of-the-art CNC Diamond Machine lathe is shown in Figure 1.

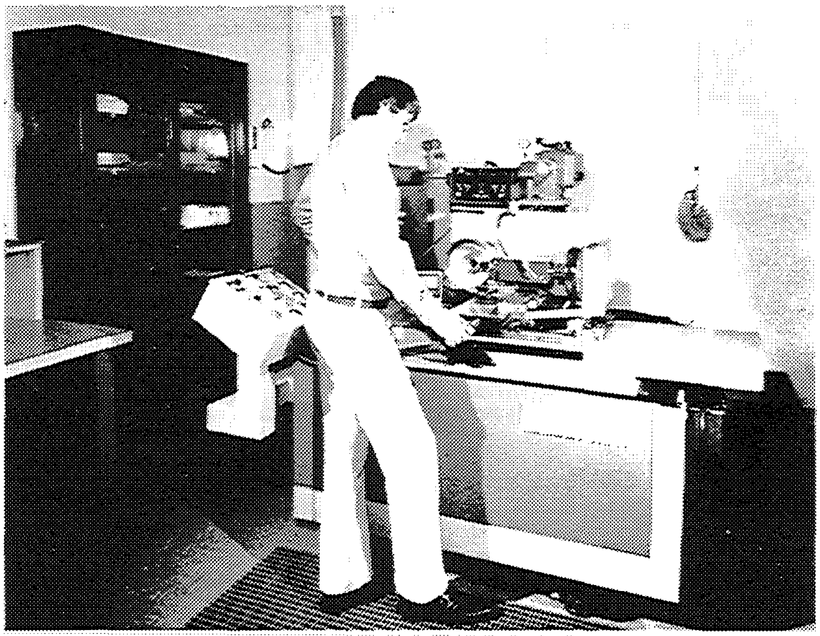

Figure 1 Diamond Tool Lathe

The increased use of diamond machined optics requires that unambiguous and accepted methods of specifying these surfaces be developed. The development of specifications presents problems because the character of diamond machined surfaces is fundamentally different from surfaces produced by conventional optical fabrication methods.

We can understand the difference in surface character and the different specification methods required by examining a rotationally symmetric spherical or aspheric surface, cut on a lathe.

The most obvious characteristic of this model surface is the phonograph record or circular diffraction grating appearance (Figure 2). This appearance is due to the cutting tool lead, and occurs at a spatial period equal to the tool advance. The fundamental period pattern is easily visible, particularly because of its high spatial correlation.

There are similar, higher frequency errors due to minor imperfections on the cutting tool edge. Lower frequency errors are due to lead screw periodicity, as well as periodic and occasional irregularities in the machine ways. The degree of correlation of these errors is less than that due to the lead screw, but substantially higher than the microirregularities present on conventionally polished surfaces.

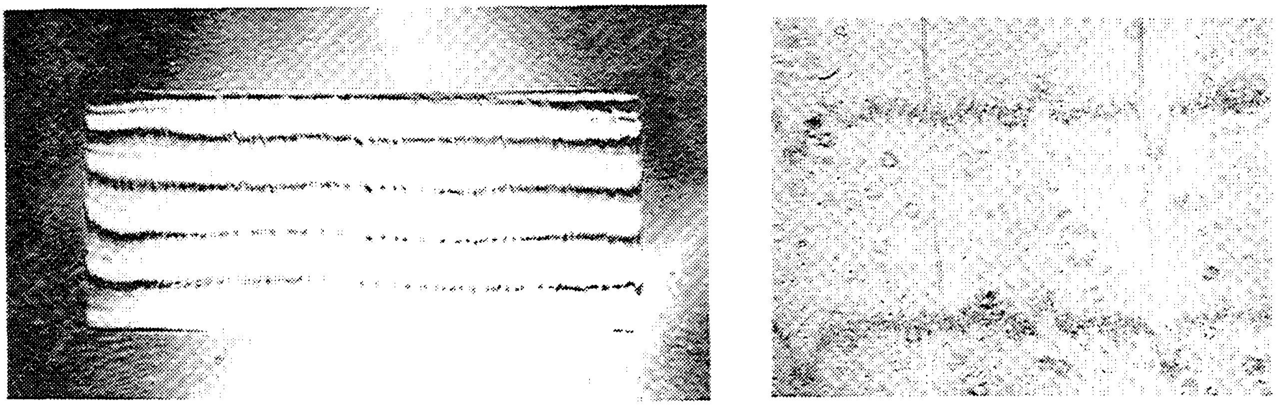

Figure 2 Interferogram of Diamond Turned Spin Mirror

We will address the optical system performance effects due to these surface imperfections, so that a structure for optical surface specification can be developed. It is clear to us that there is no single or simple method for specification that will satisfy designers, users and manufacturers. However, we have attempted to define an approach which should prove useful.

The effects of figure errors (macroscopic geometrical errors) are presented first, followed by an examination of micro-topography effects. Methods for defining these errors in the form of specifications are then presented. Finally, we point out where we believe that additional work is warranted.

Surface Error Categories

The figure errors of diamond turned optics may be classified into three categories (Figure 3):

1. Low frequency errors - conventional aberrations 0–5 cycles/radius
2. Middle frequency errors - "slope errors" 5 cycles/radius to 100 wavelength period
3. High frequency errors - "microroughness" 100 wavelengths period and shorter.

We will categorize the first two as figure errors and the last as microtopography.

This subdivision is somewhat superficial, but it does help in understanding the mechanisms which produce these errors. For example, gross systematic errors in the control system for the diamond tool would produce low frequency errors, as would warping of the workpiece on the lathe. Vibration, tool feed rate, tool imperfections and similar effects are manifest in the middle and high frequency regions.

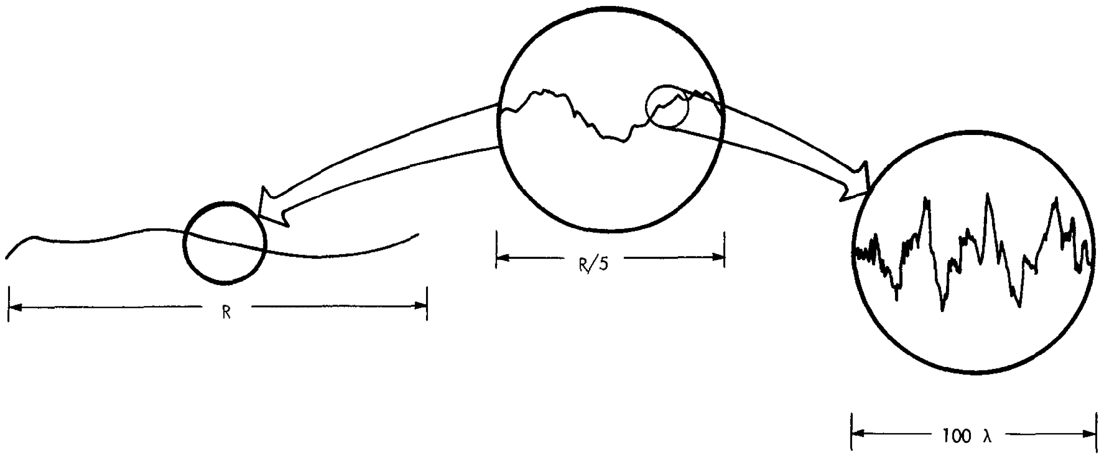

Figure 3 Surface Error Categories

The high frequency errors found in diamond turned surfaces are generally highly periodic and highly correlated as compared to the random, low correlation roughness found in conventionally ground and polished surfaces. Also, diamond turned surfaces have a high degree of symmetry as opposed to the isotropic randomness of ordinary optics.

Figure Errors

Measurement and characterization of low frequency errors into the classical aberrations is an old and practiced art, and is no different for diamond turned surfaces. However, careful analysis of the mechanics of diamond turning a sphere or paraboloid shows an effect not encountered in usual optics. When turning a surface of revolution, a common error is decentration of the tool on the workpiece: the origin of the tool's coordinate system does not lie on the axis of the lathe (Figure 4). We find that for a small amount of decentration, the figure error is approximately

$$\Delta = \frac{x_o^2 - y_o^2}{2R} - \frac{x_o}{R}\rho, \qquad (1)$$

where x_o and y_o are decentrations in directions parallel and perpendicular to the plane of tool motion, respectively. R is the radius of the sphere or paraboloid, and ρ is radius measured from the axis of the lathe. This aberration is linear with radius, and thus describes a cone. If we mold this conical aberration into the usual scheme, it is represented primarily by defocus and first order spherical aberration accompanied by an infinite sum of higher order spherical aberrations in lesser amounts.

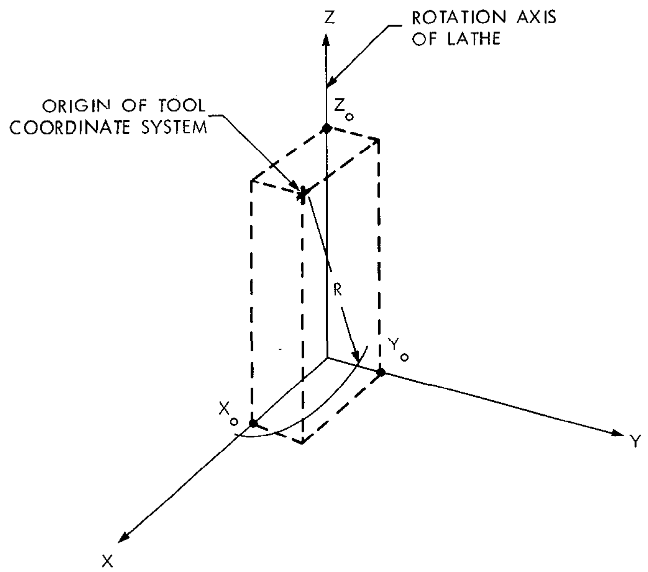

Figure 4 Geometry of Decentration Error

The geometrical effect of the defect is unusual. Figure 5 is a representation of the meridonal plane of a turned spherical surface with and without the decentration defect. A point source placed at the center of curvature of the perfect sphere will be reimaged on itself. The effect of the decentration is to produce two point images in the meridional plane, or a ring image for the rotationally symmetric surface. The diameter of the ring is four times the linear decentration of the axis.

A more detailed discussion of this defect, including the imaging effects, is currently being prepared for publication.[3]

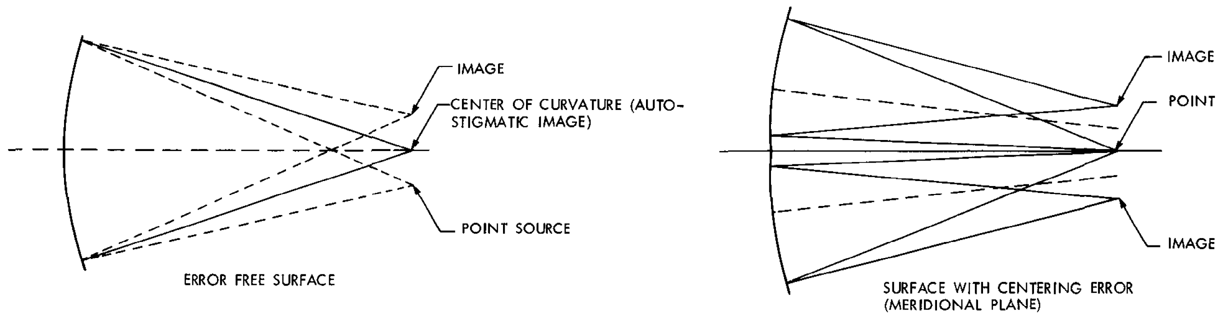

Figure 5 Effect of Tool Decentration on a Surface of Revolution

Microtopography

Perhaps the most obvious characteristic of diamond turned optics is the microscopic ripples caused by the finite feed rate of the tool, which can only be removed by postpolishing. This is a highly periodic error, and there may be other factors which cause periodic errors, such as an inaccurate lead screw. Importantly for a surface of revolution, these ripples are periodic in radius, and we may approximate them by a circularly symmetric phase diffraction grating. If we wish to evaluate* the image quality of such a surface, we may use the methods of scalar diffraction theory, or of vector diffraction theory. The scalar theory is accurate only near the center of the field, whereas the vector theory is accurate for all field angles, and accounts for the effects of polarization of the incident wave. Nevertheless, comparison of these two methods indicates that they give similar results for most cases of interest here, and we will examine the results of the scalar theory, which is mathematically more facile.

To represent the effect that ripples in a diamond turned surface of revolution have on a plane wavefront, we approximate the radial profile of the phase of the wavefront by a cosine.

The amplitude in the image plane is the Hankel transform of this pupil function,

$$u(r) = 2 \int_0^1 e^{ikA \cos 2\pi f\rho} J_0(r\rho)\rho d\rho \tag{2}$$

where $k = 2\pi/\lambda$, f and ρ are dimensionless frequency and radius in the pupil, respectively, A is the amplitude of the cosine, and r is the dimensionless radius in the image plane.[7] If we substitute the series

$$e^{ikA \cos 2\pi f\rho} = J_0(kA) + 2\sum_{n=1}^{\infty} i^n J_n(kA) \cos 2\pi n f\rho \tag{3}$$

into Eq. (2), u (r) becomes

$$u(r) = J_0(kA) \frac{2 J_1(r)}{r} + 4\sum_{n=1}^{\infty} i^n J_n(kA) \int_0^1 \cos 2\pi n f\rho \, J_0(r\rho) \, \rho d\rho \tag{4}$$

The term outside the sum is the familiar Airy pattern, multiplied by a constant. Since f is typically large, and J_0 is highly periodic with period $\sim 2\pi$, we conclude that the integral in Eq. (4) will be negligibly small except when r is nearly equal to $2\pi nf$. This result reminds one of the grating equation, and indeed we can predict that the central point image will be surrounded by a series of concentric rings with radii $r_n = 2\pi nf$. If the rings and the image do not overlap significantly, we may write the intensity (point spread function) as

$$U(r) = |u(r)|^2 \approx \left[J_0(kA)\right]^2 \left[\frac{2 J_1(r)}{r}\right]^2 + \sum_{n=1}^{\infty} \left[4 J_n(kA)\right]^2 \left[\int_0^1 \cos 2\pi n f\rho \, J_0(r\rho) \, \rho d\rho\right]^2 \tag{5}$$

We recognize from Eq. (5) that the Strehl definition is[7]

$$\mathcal{D} = \left[J_0(kA)\right]^2 \tag{6}$$

and is independent of the frequency f. If we use the Strehl definition as a specification parameter, it places a strict tolerance on the wavefront. If we demand that $\mathcal{D} \geq 0.8$, we must have the parameter $A \leq \lambda/10$. Indeed, for a mirror, the amplitude of the surface profile is $\alpha = A/2$, and the requirement is $\alpha \leq \lambda/20$. For kA equal to a root of J_0, we have the disturbing result that the point image vanishes, and all the energy is contained in the diffracted rings. At the first root of J_0, $\alpha \approx \lambda/5$.

Numerical evaluation of the transfer function of a rotationally symmetric cosine-phase pupil function[7,8] with f large shows that as A is increased, the contrast in the lower spatial frequencies is attenuated. Again, this effect is largely independent of f, except for the number of ripples in the transfer function, which is equal to 2f.

Notice that if the field of view of the optic in question is limited (e.g., by a field stop) to $r \leq \pi f$, then the diffracted rings are truncated from the point spread function and the image quality is only slightly degraded. If this is not done, a poorly diamond turned surface is capable of causing a large amount of veiling glare.

* The electromagnetic theory of diffraction will not be discussed here, but the reader is directed to References 4–6.

Specification Format

The principal purpose of a surface specification is to assure optical system performance. The specification should be easily measurable and relatable to the variables of the fabrication process. In many cases, it is not possible to satisfy the user and manufacturer with a single specification, so that a certain redundancy must exist. This is especially true for a diamond machined surface, where optical performance must be related to machine shop practice.

We have found it useful to consider surface specification for two aspects of system performance: image quality and light scattering.

Image Quality

Image quality requirements are determined from a system error budget, usually in terms of an Optical Transfer Function (OTF). The allowable surface figure errors are determined from the OTF by conventional methods. The surface figure errors are then stated in terms of an amplitude spectrum of surface error. The effects of microripple, determined as previously discussed are included in the high spatial frequency portion of the amplitude spectrum.

A typical surface specification (Figure 6) is seen to be divided into three regions corresponding to the error spatial frequency categories we have chosen. The specification may be interpreted in terms of machine characteristics, control errors and machine setup.

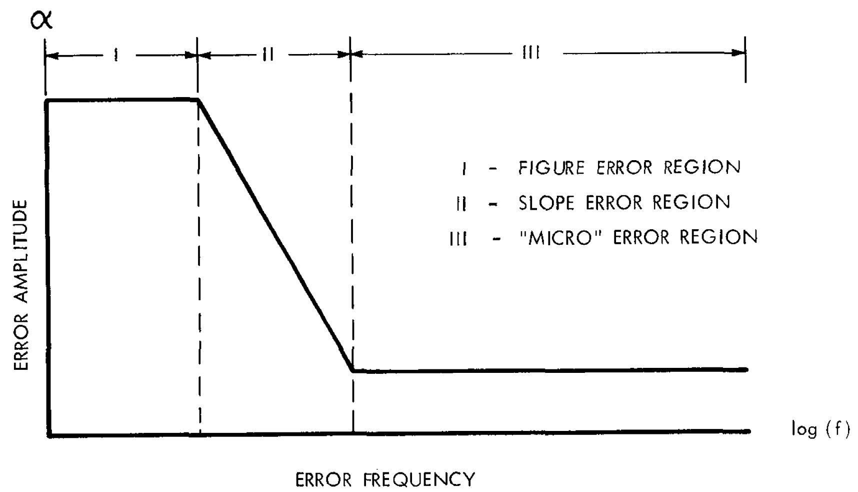

Figure 6 Typical Error Budget for Diamond Turned Mirror - Amplitude Spectrum of Surface Error

The slope error (region II) is merely a restatement, in frequency space, of the optical surface slope specification usually stated as "waves per cm." The purpose of the specification is to control the geometric ray reflections.

For example, (refer to Figure 7), a cutting tool of radius r_o will produce a cusp of height h, which is related to the tool advance a, by the expression

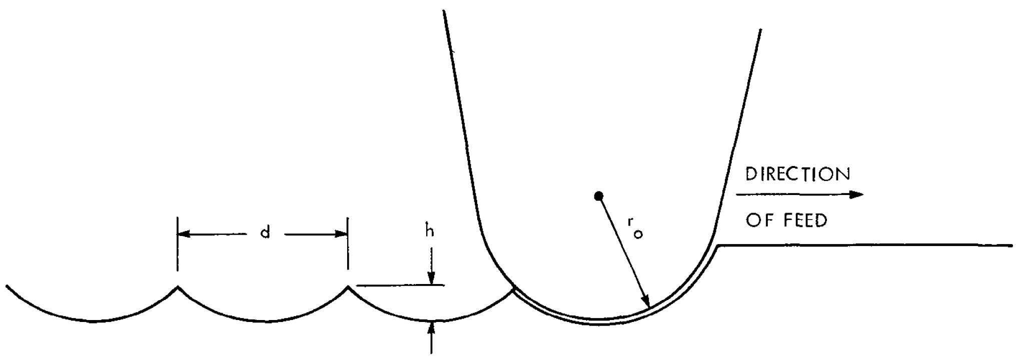

Figure 7 Cusp Geometry

$$h = \frac{2r_o + \sqrt{4r_o^2 - \frac{a^2}{4}}}{2} \tag{7}$$

or for $a \ll r_o$,

$$h \cong \frac{a^2}{8r_o} \tag{8}$$

So that for $r_o = 5$ mm and $a = 0.05$ mm, the cusp height will be 6.3×10^{-5} mm, at a frequency of 20 mm^{-1}.

The machine operator may adjust the cusp height by varying the tool advance in order to conform to the specification.

Light Scattering

The scattering from a diamond turned surface is characterized by the peak in the angular scatter due to the periodic structure of the surface.

Bennett[9] has described a hierarchy of testing, (Table I) in order of decreasing specificity, for scattering. This same hierarchy is applicable to specifying surfaces. That is, specify the surface quality to determine the minimum level of testing. The quantities or functions determined by these tests are mathematically related to each other, with varying degrees of ambiguity.

Table I SCATTERED LIGHT TEST HIERARCHY (SPECIFICITY)

FUNCTIONAL SYSTEM TEST
BRDF MEASUREMENT
TOTAL INTEGRATED SCATTER (TIS) MEASUREMENT
RMS ROUGHNESS
SCRATCH AND DIG
(FROM H. BENNETT)

We recommend specifying and testing the quantity desired and would not permit inferring one from another.

The general topic of specifying scattering was discussed at great length at the NBS Conference on Standards from Scattering from Optical Surfaces. This conference has been summarized by Young.[10]

Conclusions

We have attempted to present a framework for specifying optical surfaces manufactured by single point diamond machining. The results to date described here are far from completely useful. It is clear that a means to easily convert a surface error amplitude spectrum into optical transfer functions or other image characteristic is needed in order to completely and unambiguously specify an optical component. Further investigation is also needed with respect to the effects of these surfaces on polarized light.

The results presented should allow the tolerancing and specification of some of the errors unique to diamond machined optics.

Acknowledgements

The authors would like to express their thanks to Gene Toler and Irv Abel for many helpful discussions which took place during the evolution of the concepts expressed in this paper. We are also indebted to John Johnson for the derivation of the effects of decentration error.

References

1. Saito, T.T., "Diamond Turning of Optics: Past, Present, Exciting Future," Optical Eng. 17, 570 (1978).
2. Johnson, F., "Diamond Turning at Honeywell," Proc. SPIE 159, 72 (1978).
3. Johnson, J. et al, to be published.
4. Petit R. "Electromagnetic Grating Theories: Limitations and Successes," Nouv. Rev. Optique 6, 129 (1975).
5. Kalhor, H.A. and Neureuther, A.R, "Numerical Method for the Analysis of Diffraction Gratings," J. Opt. Soc. Am. 61, 43 (1971).
6. Kalhor, H.A. and Neureuther, A.R., "Effects of Conductivity, Groove Shape, and Physical Phenomenon on the Design of Diffraction Gratings" J. Opt. Soc. Am. 63, 1412 (1973).
7. Barakat, R and Houston, A, "The Effect of a Sinusoidal Wavefront on the Transfer Function of a Circular Aperture" Appl. Opt. 5, 1850 (1966).
8. Wetherell, W., "Ultraviolet and Visible Scattered Light Effects on the Optical Performance of the Large Space Telescope," Itek Corp. Tech Report #PFR-74-161 (1974).
9. Bennett, H,. Standards for Optical Surface Quality Using Total Integrated Scattering," Conference on Standards for Scattering from Optical Surfaces, Boulder, CO (1979) (unpublished).
10. Young, M., "Summary of Conference on Standards for Scattering from Optical Surfaces," Proc. SPIE 181 (1979).